

Supplemental Information

Expression Pattern of MAGUKs in Interneurons of the Visual Cortex

Gulcan Akgul and Lonnie P. Wollmuth

Supplemental Figure 1. The MAGUK riboprobes show high specificity for their corresponding mRNA. 2

Significance: Dot blot analysis shows that our MAGUK riboprobes hybridize specifically to their corresponding mRNA with little or no cross-hybridization.

Supplemental Figure 2. The MAGUK riboprobes have layer/cell-type specific hybridization patterns in the adult mouse cerebellum. 4

Significance: In the cerebellum, MAGUKs show layer and cell-type specific expression, and our riboprobes recapitulate these findings highlighting their specificity.

Supplemental Figure 3. Characterization of rabbit anti-PV on mouse tissue. 5

Significance: Cell-type specific staining of the cortex, hippocampus and cerebellum in wild type and transgenic mouse tissue is consistent with previous results.

Supplemental Figure 4. Characterization of rat anti-SOM on mouse tissue. 7

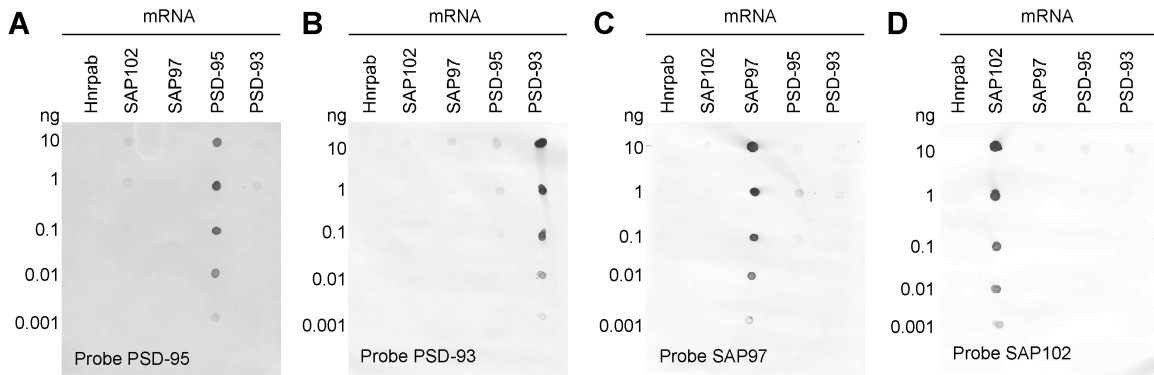
Significance: Cell-type specific staining of the cortex, hippocampus and cerebellum in wild type and transgenic mouse tissue is consistent with previous results.

Supplemental Figure 5. Double labeling of the mouse cortex with rabbit anti-PV and rat anti-SOM. 9

Significance: Although not explored in detail, in our limited data set where we double labeled visual cortex with anti-PV and anti-SOM, we did not find any overlap, consistent with previous results.

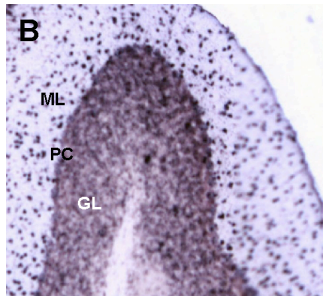
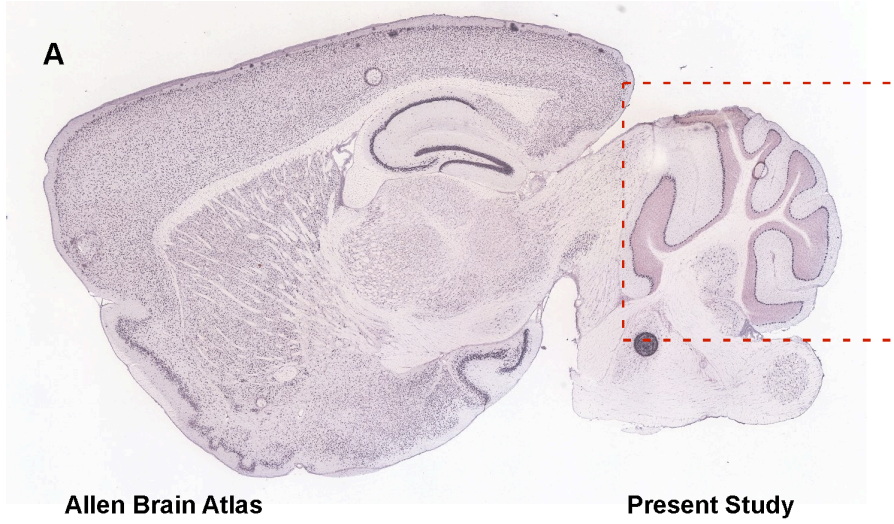
Supplemental Figure 6. SAP97 mRNA expression in layer 5 of the juvenile (P15) mouse visual cortex. 10

Significance: As in layers 2/3 (Figures 5 & 6), SAP97 is highly expressed in layer 5 PV+ and SOM+ interneurons.

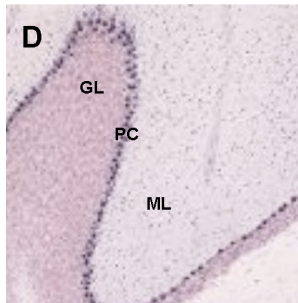
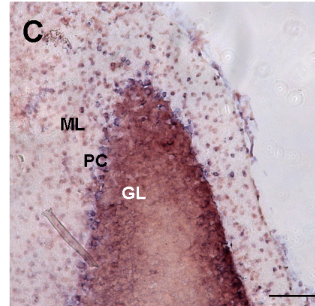


Supplemental Figure 1. The MAGUK riboprobes show high specificity for their corresponding mRNA.

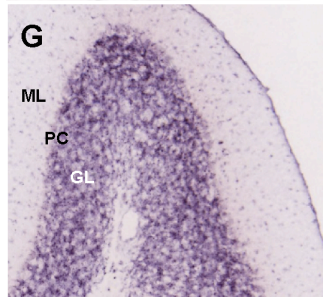
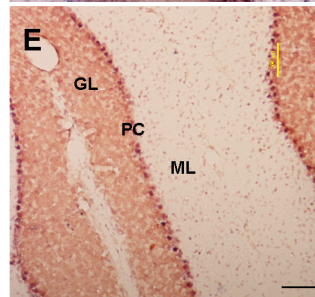
Nylon membranes (Ambion, Austin, TX) (A-D) were dot-blotted with gradients (0.001-10 ng) of MAGUK and Hnrpab (as a negative control) mRNAs. Membranes were hybridized with either DIG-labeled PSD-95 (A), PSD-93 (B), SAP97 (C) or SAP102 (D) riboprobes. Anti-DIG-AP fragments (1:1000) and NBT/BCIP (Roche Applied Science, Indianapolis, IN) were used to develop hybridization signal. Dark spots on each membrane show successful hybridizations between the probe and the mRNA. Note that the intensity of the spots changes in a concentration dependent manner with the spots largely restricted to a riboprobe and its corresponding mRNA. Full length MAGUK and *X. laevis* Hnrpab mRNAs were transcribed *in vitro* with mMACHINE™ Kit (Ambion, Austin, TX). RNA concentrations were determined with SmartSpec™ 3000 Spectrophotometer (Bio-Rad, Hercules, CA).



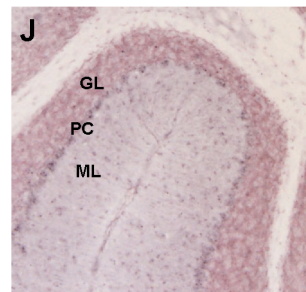
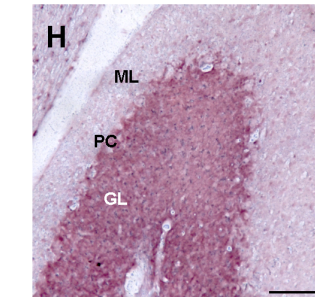
PSD-95
(Dlgh4)



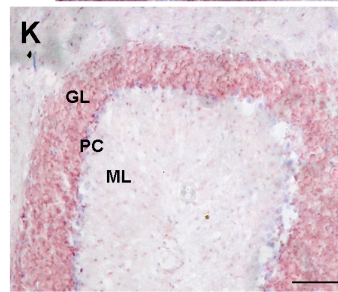
PSD-93
(Dlgh2)



SAP97
(Dlgh1)



SAP102
(Dlgh3)

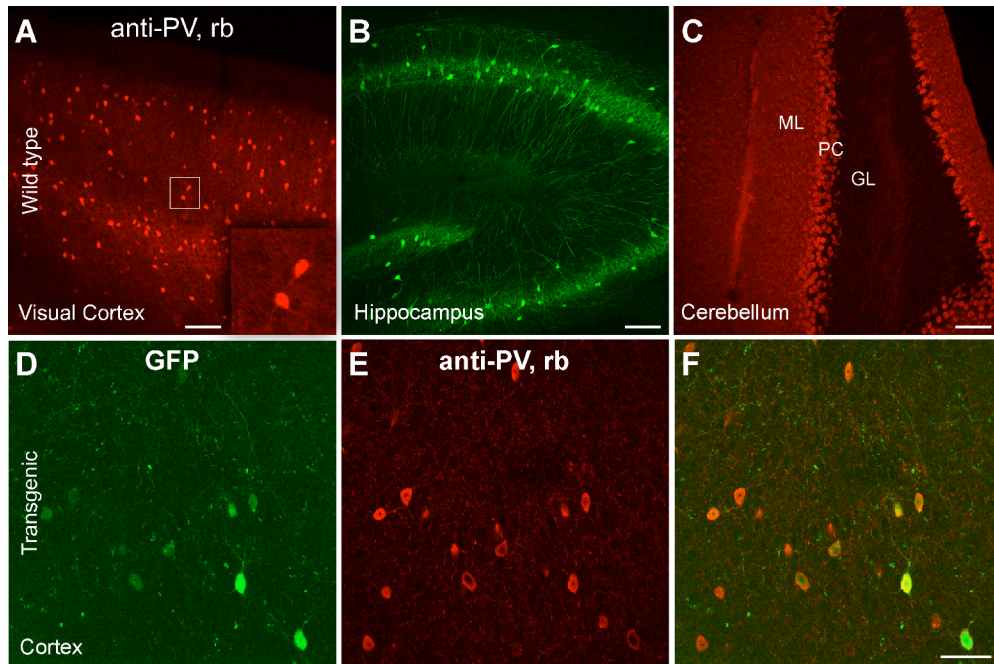


Supplemental Figure 2. The MAGUK riboprobes have layer/cell-type specific hybridization patterns in the adult mouse cerebellum.

All tissue sections shown are from adult mouse cerebellum either the Allen Brain Atlas (<http://mouse.brain-map.org>) (left column; A, B, D, F, H) or the present study (right column; C, E, G, I). The cerebellar layers are marked: molecular layer (ML), Purkinje cell layer (PC) and granule cell layer (GL).

Left column: In situ hybridization images of a whole sagittal brain section labeled with PSD-93 riboprobe (A) or enlarged images of the cerebellum labeled with PSD-95 (B), PSD-93 (D), SAP97 (F) or SAP102 (H) riboprobes. Hybridization signals were detected chromogenically.

Right column: In situ hybridization images are labeled with PSD-95 (C), PSD-93 (E), SAP97 (G) or SAP102 (I) riboprobes used in the present study. Hybridization signals were detected chromogenically (see Materials & Methods). Our four MAGUK riboprobes show layer and cell type specific expression comparable to that seen in the Allen Brain Atlas images as well as that published previously for in situ hybridization (Muller et al., 1995; Brenman et al., 1996; Chetkovich et al., 2002). The PSD-95 riboprobes shows strong, diffuse labeling in the granule cell layer and strong cell-type expression in the molecular layer (B; cf., C) (Chetkovich et al., 2002). PSD-93 riboprobes shows strong labeling in the Purkinje cells as well as diffuse labeling in granule cell layer (D; cf., E) (Brenman et al., 1996). SAP97 riboprobes does not label Purkinje cells but does strongly label the granule cell layer (F; cf., G) (Muller et al., 1995). Although more diffuse, the SAP102 riboprobes show most prominent labeling of the granule and Purkinje cell layers (H; cf., I). Scale bar, 100 μ m.



Supplemental Figure 3. Characterization of rabbit anti-PV on mouse tissue.

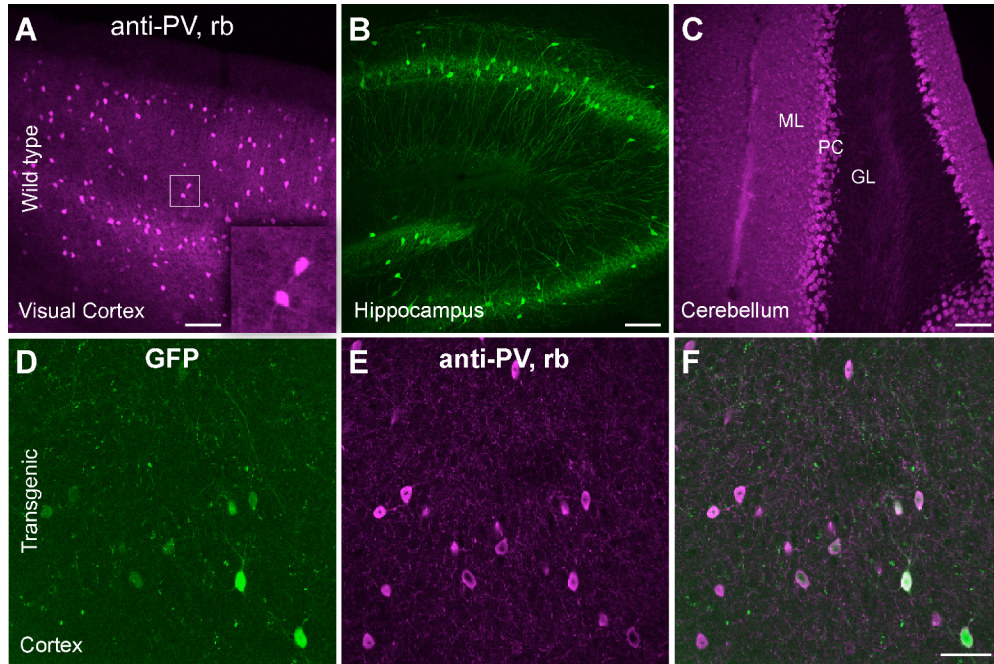
Cell-type specific staining of the cortex, hippocampus and cerebellum in wild type and transgenic mouse tissue is consistent with previous results.

Tissue sections were obtained from wild type (A-C) or transgenic (D-F) mouse brains and labeled with rabbit anti-PV. 50 μm floating sections were blocked with 10% normal serum at room temperature for 1 hour and probed with the primary antibody at room temperature overnight.

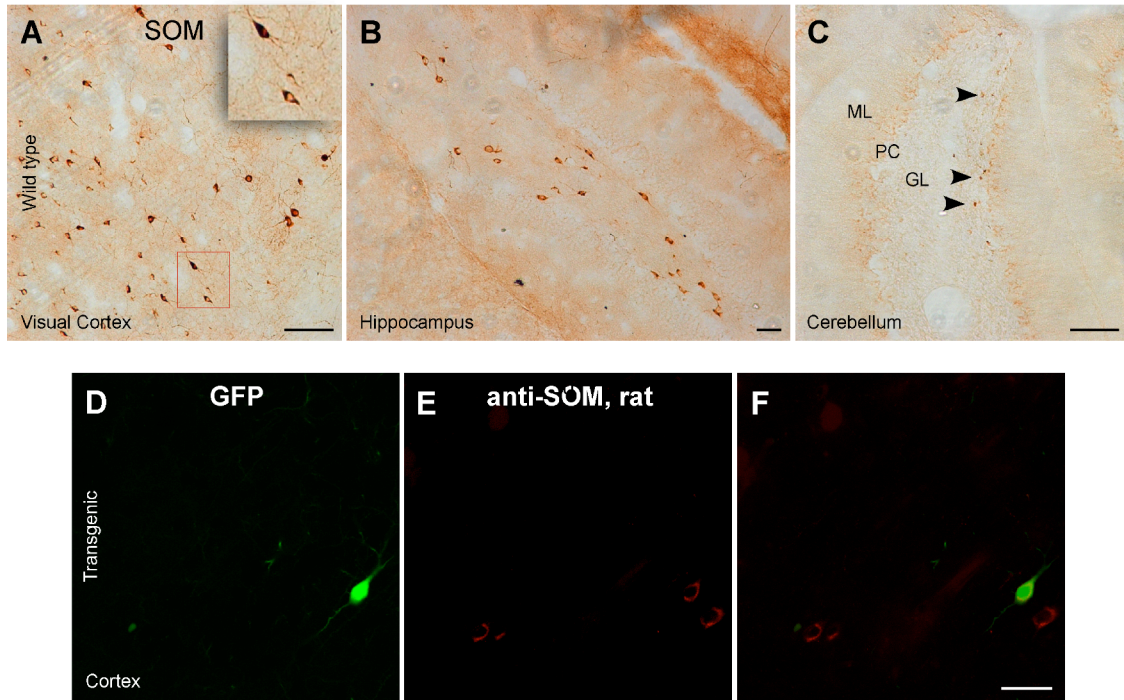
(A-C) Low magnification images show PV staining in the visual cortex (A), the hippocampus (B), and the cerebellum (C) (ML, molecular layer; PC, Purkinje cell layer; GL, granule cell layer). Immunofluorescent labeling is consistent with previous studies: In the cortex (Kawaguchi and Kubota, 1993; Gonchar et al., 2007), there is widespread labeling of interneurons; in the hippocampus (Dun et al., 1994), labeling is mainly restricted to the pyramidal layer as well as dentate gyrus; and in the cerebellum (Schneeberger et al., 1985), there is labeling of Purkinje and basket (ML) cells. Scale bar, 100 μm .

(D-F) The heterozygous transgenic mice (B13) express GFP in a subset of PV+ interneurons (Dumitriu et al., 2007). (D) Green cells in the transgenic mouse cortex are GFP expressing PV+ interneurons. (E) Red cells in the same tissue section are PV immunopositive neurons. The merge image (F) shows the overlap of GFP expression and antibody labeling. Consistent with previous results (Dumitriu et al., 2007), rabbit anti-PV stains every GFP expressing neuron and additional cells in the cortex (D-F) as well as in the hippocampus and cerebellum (data not shown).

We also found no labeling of any neurons/cells in the cortex of P10 animals (data not shown), consistent with the onset of parvalbumin expression, which is around P14, in the cortex (e.g., Gonchar et al., 2007). Scale bar, 50 μm .



Supplemental Figure 3 (in magenta-green).



Supplemental Figure 4. Characterization of rat anti-SOM on mouse tissue.

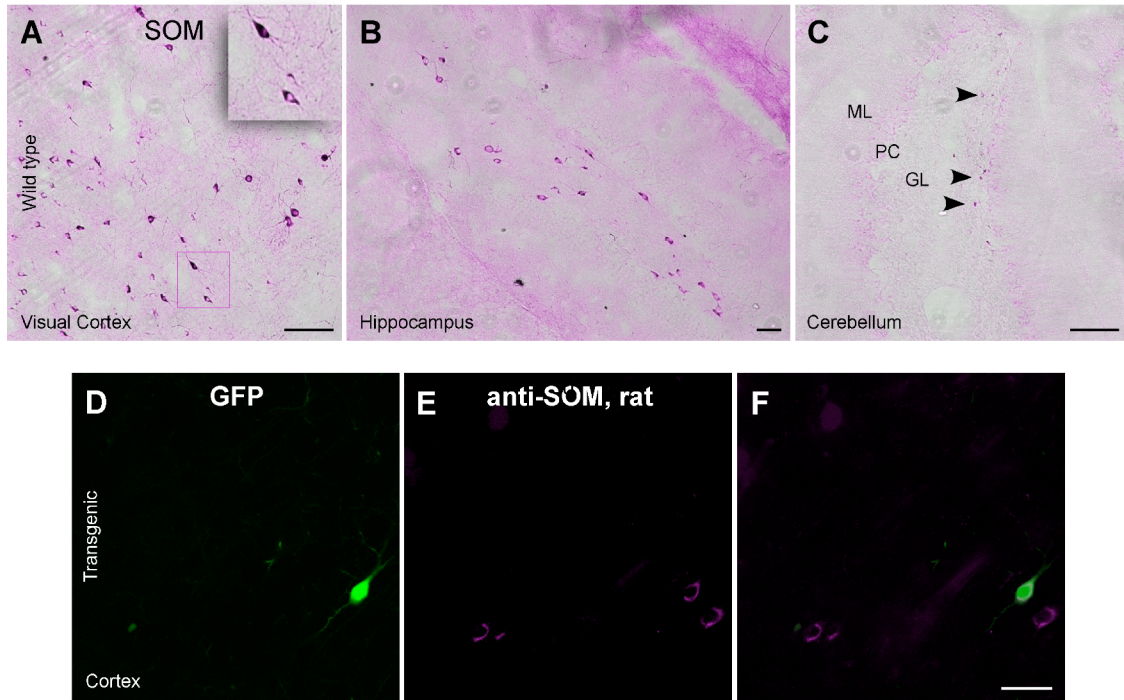
Cell-type specific staining of the cortex, hippocampus and cerebellum in wild type and transgenic mouse tissue is consistent with previous results.

Tissue sections were obtained from wild type (A-C) or transgenic (D-F) mouse brains and labeled with rat anti-SOM.

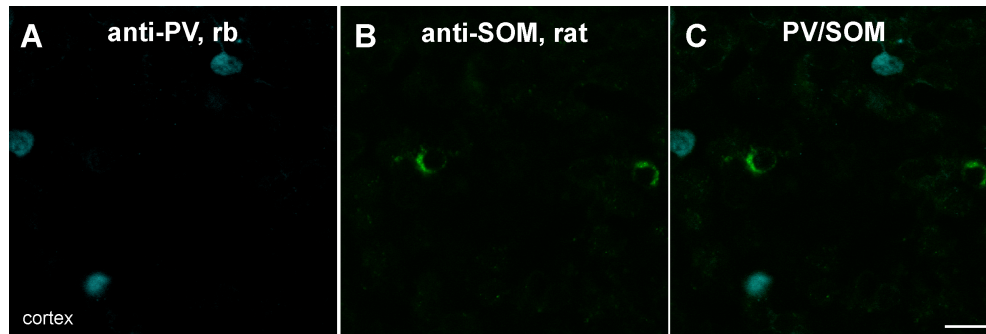
(A-C) Brightfield images show SOM staining in the visual cortex (A), the hippocampus (B), and the cerebellum (C) (see Supplemental Figure 3 for additional details).

Immunolabeling is consistent with previous results: In the mouse cortex (e.g., Kubota et al., 1994), there is widespread labeling of interneurons with known morphology (e.g., bitufted enlarged inset); in the hippocampus (Dun et al., 1994), there is dispersed labeling in the hilus; in the cerebellum (Geurts et al., 2001), only a few small cells are labeled in the granular layer (C).

(D-F) anti-SOM was tested on transgenic mouse tissue, in which a subset of SOM+ interneurons are expressing GFP (Oliva et al., 2000). Green cell on the confocal images of the section of transgenic mouse cortex is a GFP expressing SOM+ interneuron (D), and red cells on the same tissue section are SOM immunopositive neurons (E). Consistent with previous results (Oliva et al., 2000), rat anti-SOM stains every GFP expressing neuron and additional cells in the cortex (D-F) as well as in the hippocampus (data not shown). Scale bar, 50 μ m.



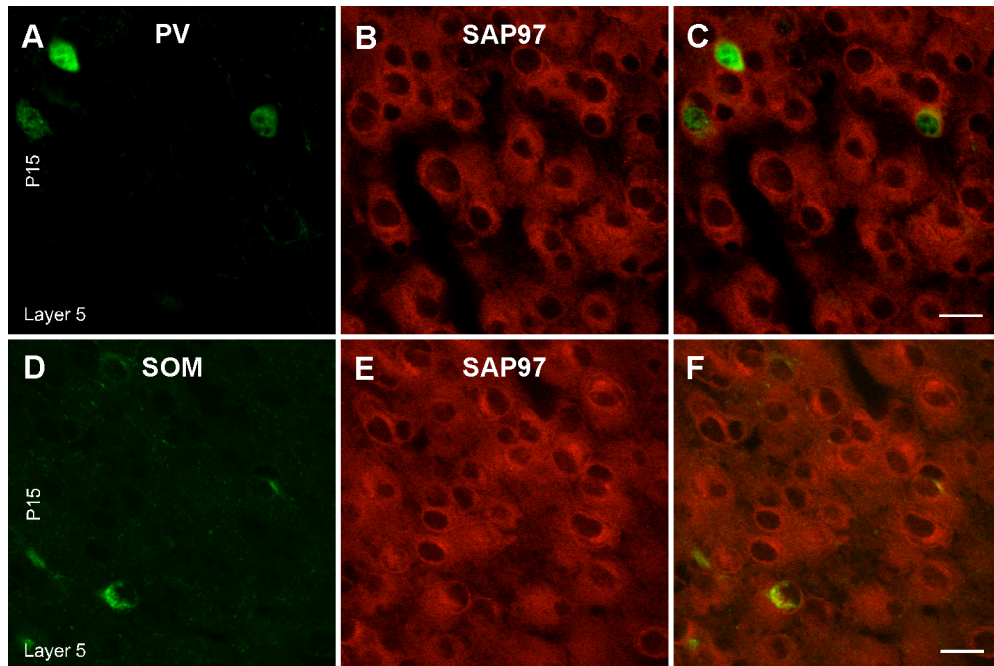
Supplemental Figure 4 (in magenta-green).



Supplemental Figure 5. Double labeling of the mouse cortex with rabbit anti-PV and rat anti-SOM.

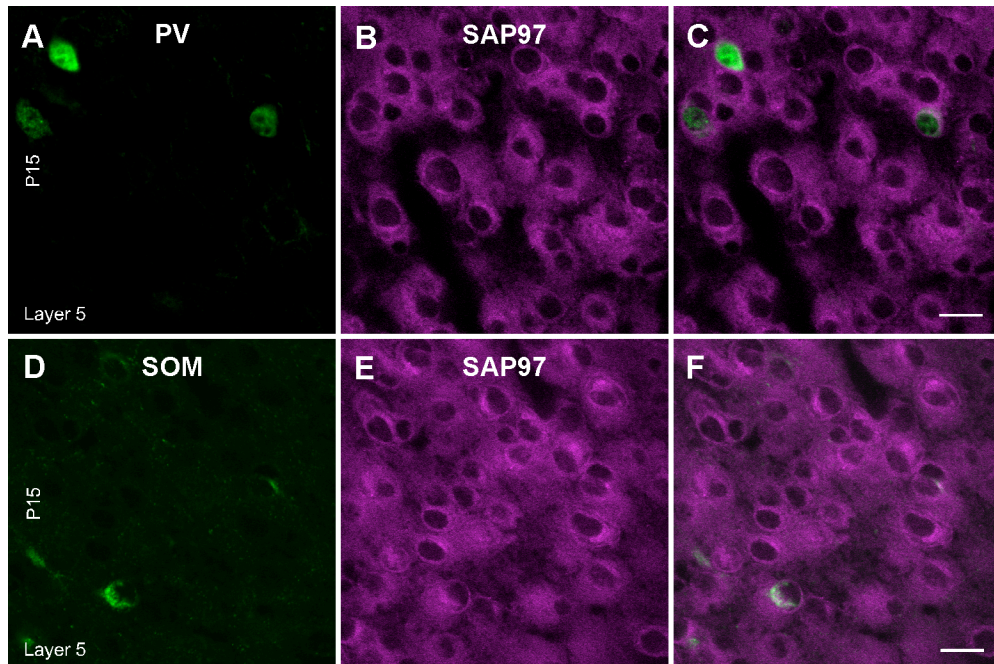
No apparent overlap in the visual cortex between anti-PV and anti-SOM.

Tissue sections were obtained from wild type mouse cortex and double immunostained. (A) Sections were labeled with rabbit anti-PV (blue). (B) The same sections were labeled with rat anti-SOM (green). As shown in the merged image (C), there is no obvious overlap between the two probes consistent with previously published data (Kubota et al., 1994; Gonchar et al., 2007). Images are magnified at 63X. Scale bar, 20 μm .



Supplemental Figure 6. SAP97 mRNA expression in layer 5 of juvenile (P15) mouse visual cortex.

Tissue sections were obtained from juvenile (P15) mouse brains. In the left column, sections were labeled with either rabbit anti-PV (A) or rat anti-SOM (D) (green). Middle column (B, E), the same sections were hybridized with DIG-labeled SAP97 riboprobe (red). Right column (C, F) shows merged images. Images are at 63X. Scale bar, 20 μ m.



Supplemental Figure 6 (in magenta-green).

Supplemental References

- Brenman JE, Christopherson KS, Craven SE, McGee AW, Bredt DS (1996) Cloning and characterization of postsynaptic density 93, a nitric oxide synthase interacting protein. *J Neurosci* 16:7407-7415.
- Chetkovich DM, Bunn RC, Kuo SH, Kawasaki Y, Kohwi M, Bredt DS (2002) Postsynaptic targeting of alternative postsynaptic density-95 isoforms by distinct mechanisms. *J Neurosci* 22:6415-6425.
- Dumitriu D, Rosa C, Huang J, Yuste R (2007) Correlation between axonal morphologies and synaptic input kinetics of interneurons from mouse visual cortex. *Cerebral Cortex* 17.
- Dun NJ, Dun SL, Wong RK, Forstermann U (1994) Colocalization of nitric oxide synthase and somatostatin immunoreactivity in rat dentate hilar neurons. *Proc Natl Acad Sci U S A* 91:2955-2959.
- Geurts FJ, Timmermans J, Shigemoto R, De Schutter E (2001) Morphological and neurochemical differentiation of large granular layer interneurons in the adult rat cerebellum. *Neuroscience* 104:499-512.
- Gonchar Y, Wang Q, Burkhalter A (2007) Multiple distinct subtypes of GABAergic neurons in mouse visual cortex identified by triple immunostaining. *Front Neuroanat* 1:3.
- Kawaguchi Y, Kubota Y (1993) Correlation of physiological subgroupings of nonpyramidal cells with parvalbumin- and calbindinD28k-immunoreactive neurons in layer V of rat frontal cortex. *J Neurophysiol* 70:387-396.
- Kubota Y, Hattori R, Yui Y (1994) Three distinct subpopulations of GABAergic neurons in rat frontal agranular cortex. *Brain Res* 649:159-173.
- Muller BM, Kistner U, Veh RW, Cases-Langhoff C, Becker B, Gundelfinger ED, Garner CC (1995) Molecular characterization and spatial distribution of SAP97, a novel presynaptic protein homologous to SAP90 and the *Drosophila* discs-large tumor suppressor protein. *J Neurosci* 15:2354-2366.
- Oliva AJ, Jiang M, Lam T, Smith K, Swann J (2000) Novel hippocampal interneuronal subtypes identified using transgenic mice that express green fluorescent protein in GABAergic interneurons. *J Neurosci* 20.
- Schneeberger PR, Norman AW, Heizmann CW (1985) Parvalbumin and vitamin D-dependent calcium-binding protein (Mr 28,000): comparison of their localization in the cerebellum of normal and rachitic rats. *Neurosci Lett* 59:97-103.